

Experimental limits on the existence of strongly interacting massive particles bound to gold nuclei

D. Javorsek II,¹ D. Elmore,¹ E. Fischbach,¹ T. Miller,¹ D. Oliver,² and V. Teplitz³

¹*Department of Physics, Purdue University, West Lafayette, Indiana 47907*

²*Department of Geological Sciences, Southern Methodist University, Dallas, Texas 75275*

³*Department of Physics, Southern Methodist University, Dallas, Texas 75275*

(Received 19 December 2000; published 8 June 2001)

We report the results from an experimental search for strongly interacting massive particles bound to gold nuclei. A scan for heavy gold isotopes with masses ranging from 186.3 to 325.9 GeV/ c^2 was performed on laboratory gold and gold from western Australia using PRIME Lab, the Purdue Accelerator Mass Spectrometer facility. The results provide significant new constraints on current models which predict the existence of such particles with abundance ratios in the range 10^{-11} – 10^{-10} .

DOI: 10.1103/PhysRevD.64.012005

PACS number(s): 14.80.-j, 26.35.+c, 82.80.Ms, 95.35.+d

A number of recent theoretical arguments have raised the possibility that there exist in nature strongly interacting massive particles (SIMPs) [1–14]. These particles are typically stable neutral fermions, and their existence could help to resolve a number of outstanding problems, as we discuss below. Since any new strongly interacting particle could in principle bind to nuclei, SIMPs could manifest themselves as superheavy isotopes of ordinary elements. We report here the results of a recent search for SIMPs bound to gold nuclei, forming a new isotope of ^{79}Au denoted by ^{79}X with mass M_X , where gold has been chosen for several reasons: To start with, previous searches have focused on SIMPs bound to light nuclei [15,16], but no comparable limits exist for heavy nuclei. Moreover, SIMPs may bind preferentially to heavy nuclei, since the presence of a larger (in radius) nuclear potential well implies a smaller kinetic energy (and hence more binding) via the uncertainty principle [3]. In addition, gold can be found in sites relatively close to the surface of the Earth, where the extent of exposure of the gold to SIMPs can be estimated using geological considerations. Finally, gold readily forms negative ions, which a tandem electrostatic accelerator requires in the initial acceleration stage.

There are both particle physics and cosmological motivations for the existence of SIMPs. These include the dark matter problem [1–5], predictions of gauge mediated supersymmetry (SUSY) models [6–11], and predictions of models that explain perplexing ultrahigh-energy cosmic ray (UHECR) events [11–14]. Each of the above theories raises the possibility of SIMPs existing in nature, and each predicts a range for the SIMP mass, M_S .

SIMP models that predict saturation of the upper bound on (galactic halo) dark matter are restricted by a number of experiments as reviewed by Starkman *et al.* [17]. The relic SIMP abundance is roughly proportional to $(\sigma_{\bar{S}S}M_S)^{-1}$ where M_S is the SIMP mass and σ is the particle-antiparticle annihilation cross section [18]. As $\sigma_{\bar{S}S}$ moves beyond $\sigma_{\bar{S}S}^{\text{min}} \sim 10^{-36} \text{ cm}^2$, the bound is not saturated and the limits of Ref. [17] do not apply.

Supersymmetry (SUSY) provides another motivation for SIMPs. Raby [7] has proposed a class of SUSY models in which the gluino is the lightest supersymmetric particle (LSP), and predicts a mass range from 6.3 GeV/ c^2 to 100 GeV/ c^2 . Berezhinsky and Kachelreiss [9] suggest the

gluino is disfavored below 150 GeV/ c^2 and predict a range for the gluino mass to be 150–9000 GeV/ c^2 .

Finally, SIMPs may explain the existence of ultrahigh-energy cosmic ray events which exceed the bound of Greisen [19] and Zatsepin and Kuz'min [20] (GZK) which is 5×10^{19} eV. Albuquerque, Farrar, and Kolb [12], through analysis of air showers produced by ultrahigh-energy cosmic rays, show that the SIMP mass must be below 50 GeV/ c^2 to be consistent with the highest energy events observed and yet remain undetected. A summary of some of the theoretical predictions for SIMP mass ranges overlapping with that covered by this experiment are provided in Table I.

In the present experiment a scan for massive isotopes of Au was performed on lab gold and gold extracted from the Laverton area of western Australia (Lat. 28° 37.5' S/Long. 122° 24.0' E). The Australian gold was obtained from a depth of less than 15 cm from the surface using a metal detector. Because of its arid climate, low topographic relief, and tectonic quiescence, samples from western Australia have one of the longest near-surface exposures of any gold on Earth. We estimate that samples from western Australia have a mean near-surface residency time in excess of 40×10^6 years.

The gold samples were introduced to the ion source of the accelerator mass spectrometer (AMS) at PRIME Lab, the Purdue Rare Isotope Measurement Laboratory [21]. In the ion source energetic Cs⁺ atoms sputter the exposed gold surface, knocking the atoms off the surface and forming the Au[−] beam. At the terminal, the Au[−] and any contaminants in the beam passed through an argon stripper which removed 8 electrons. The effect of the stripping stage is twofold: Molecular contaminants in the beam which end up in the +7

TABLE I. Summary of predicted SIMP masses M_S constrained by the present experiment. For a more extensive discussion of SIMP models see Ref. [17].

Reference	Predicted SIMP masses
Mohapatra [3]	$M_S < 100 \text{ GeV}/c^2$
Raby [7]	$6.3 \text{ GeV}/c^2 < M_S < 100 \text{ GeV}/c^2$
Berezhinsky [9]	$150 \text{ GeV}/c^2 < M_S < 9 \text{ TeV}/c^2$
Albuquerque [12]	$10 \text{ GeV}/c^2 < M_S < 50 \text{ GeV}/c^2$
Starkman [17]	$3 \text{ GeV}/c^2 < M_S < 10 \text{ TeV}/c^2$

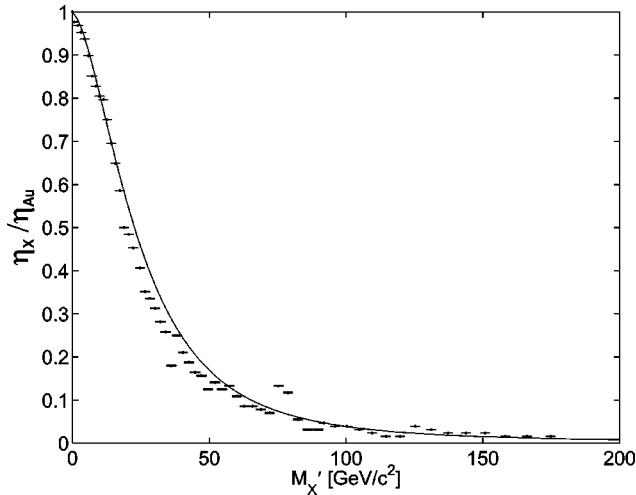


FIG. 1. Dependence of the ratio of the transmission efficiencies η_X/η_{Au} on the effective SIMP mass M'_X . η is defined as the ratio of the current at the detector to the current at the ion source. The dependence of η on M'_X arises from its dependence on the particle velocity which is a function of M'_X . The curve is a best fit to the experimental data.

charge state dissociate into individual atoms as a result of a “Coulomb explosion,” and this has the effect of significantly reducing molecular interference with any putative signal. Second by changing the sign of the charge, stripping allows the tandem to accelerate Au atoms both into and out of the accelerator. The remaining positively charged atomic ions are then accelerated to their final energy. After the accelerator a series of magnetic and electrostatic fields bends the ion beam and selects the desired isotope mass.

Finally, the energy of the ions in the beam is measured in a gas ionization detector [22]. The heavy ions enter the detector through a thin Mylar film and are introduced into a region containing low pressure propane gas and a transverse electric field. As the ions travel through the gas, they produce electron-ion pairs which separate and induce voltage signals on the cathode and anode inside the detector. The anode is subdivided into segments which determine the energy deposited over a corresponding section of the ion path, while the cathode provides a signal proportional to the total ion energy.

The gold samples were placed in cathodes attached to a wheel, which allowed each sample in turn to be rotated into the path of the Cs^+ beam. The accelerator was tuned to select for a particular mass, and after both samples were counted at this mass for 1 minute the injector magnetic field was increased, while the terminal voltage and the electric field in the electrostatic analyzer were decreased, to select for the next isotope mass. The fields in the analyzing magnets following the accelerator were held constant at their maximum values and the mass was selected by lowering the ion energy. Since the AMS is capable of resolving a mass spread of 2 unified atomic mass units (u) in the detector, we searched for heavy Au isotopes with mass M_X in 2 u steps up to a maximum mass of $325.9 \text{ GeV}/c^2$ (350 u). This maximum was determined by the observation that for higher masses the energy of the massive particles was insufficient to

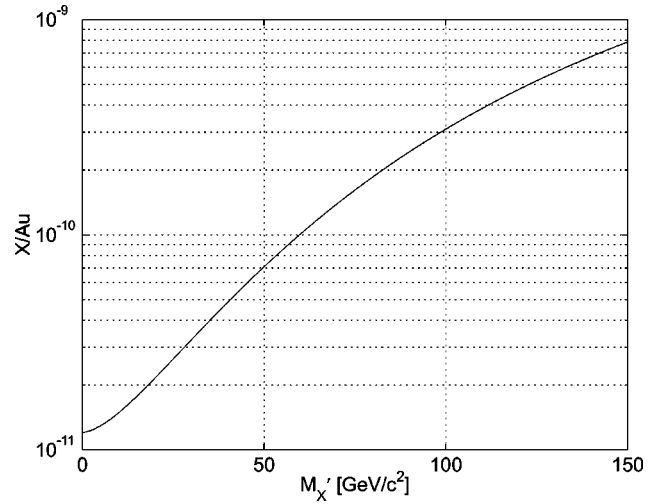


FIG. 2. 95% confidence limits on the X/Au ratio in Eq. (1) as a function of M'_X in GeV/c^2 , obtained from the Australia gold sample. As can be seen from Table II, the results for the samples of lab gold and Australian gold are virtually identical.

penetrate the Mylar window (which removes $8.2 \pm 0.2 \text{ MeV}$ from the particle’s energy) into the detector and give a reliable total energy measurement.

All magnetic components of the AMS select for a particle with a predetermined value of ME/q^2 , while electrostatic components select for E/q , where M , E , and q are the ion mass, energy, and charge, respectively. It then follows that the combination of the magnetic and electric components selects particles on the basis of M/q , so that all particles with (approximately) the same M/q will reach the detector. This observation allows us to use atomic or molecular ions in appropriate charge states as “guide beams” to tune the optics of the AMS. For example, gold ($M=197 \text{ u}$) in charge state $q=+5$ is a guide beam to test the tune of the AMS at $M_X=276 \text{ u}$ running at charge state $q=+7$ (the charge state the accelerator components were set for). Since each Au beam has a different total energy, we can distinguish the guide beams from any anomalously heavy gold nuclei by using the energy measurements made by the detector.

The efficiency of the AMS in detecting heavy nuclei is directly related to the stripper yield for each charge state. This relationship is a Gaussian-like distribution centered on an optimal charge state and is determined by the properties of the stripping gas and the incident particle. In the region of this distribution in which our experiment was performed, increasing the charge state decreases the efficiency. Theoretical studies of such charge exchange, and the resulting equilibrium charge distributions have been analyzed for more than sixty years [23]. Although theoretical calculations of the charge-changing cross sections are difficult for many electron atoms, one result is clear: the stripper yield increases with the particle’s velocity, which should be comparable to the Bohr velocity for electrons to be efficiently removed from the ion. During the scan a more massive particle has a lower velocity and thus its yield in a given charge state decreases with increasing mass. It follows that the transmission efficiency η of the AMS is a function of the mass, and hence

TABLE II. Summary of X/Au ratios for the effective SIMP mass M'_X in GeV/c^2 . We define $M'_X \equiv M_X - M_{\text{Au}} = M_S - |E_B|$ where $|E_B|$ is the magnitude of the binding energy of the SIMP to the Au nucleus. See text for further discussion.

Sample	$M'_X=3 \text{ GeV}/c^2$	$M'_X=50 \text{ GeV}/c^2$	$M'_X=100 \text{ GeV}/c^2$	$M'_X=144 \text{ GeV}/c^2$
Lab	$<1.2 \times 10^{-11}$	$<6.9 \times 10^{-11}$	$<3.0 \times 10^{-10}$	$<6.9 \times 10^{-10}$
Australia	$<1.2 \times 10^{-11}$	$<7.1 \times 10^{-11}$	$<3.1 \times 10^{-10}$	$<7.1 \times 10^{-10}$

the final experimental limits on the abundance of heavy Au isotopes with mass M_X will also depend on M_X , as can be seen in Fig. 1.

The quantity of interest is X/Au , which is the ratio of the number of hypothetical ${}_{79}X$ particles (having a mass M_X) to the number of ${}_{79}\text{Au}^{197}$ atoms in the beam. The latter quantity is determined by the Au beam current I_{det} measured by the Faraday cup located just in front of the entrance window to the detector. Using standard Poisson statistics [24] we can express X/Au in terms of I_{det} and the value of q which is the Au charge state at which we were running:

$$\frac{X}{\text{Au}} = (2.672 \times 10^{-12}) (-\ln \varepsilon_X) \frac{q}{I_{det}} \left(\frac{\eta_{\text{Au}}}{\eta_X} \right). \quad (1)$$

Here $\varepsilon_X = (1 - \text{C.L.})$ where C.L. is the confidence limit, and $\eta_{\text{Au}} (\eta_X)$ is the transmission efficiency for detecting ${}_{79}\text{Au}^{197}$ (${}_{79}X$). The results quoted here are at the 95% C.L. which corresponds to $(-\ln \varepsilon_X) = 3.00$. The numerical coefficient in Eq. (1) is obtained by noting that when q is measured in units of the electric charge [$|e|$], and I_{det} is measured in nanoamps [nA] then

$$\begin{aligned} & \frac{q(1.602 \times 10^{-19} \text{ C})(1 \text{ nA})}{I_{det}[\text{nA}] (1 \times 10^{-9} \text{ C/sec}) (60 \text{ sec})} \\ &= \frac{q(2.672 \times 10^{-12} [\text{nA}])}{I_{det} [\text{nA}]}. \end{aligned} \quad (2)$$

TABLE III. M_X (vertical) in units of GeV/c^2 versus σ_{SN} (horizontal) in units of mb. Table entries give the predicted values of $-\log_{10}(X/\text{Au})$ obtained from Ref. [25]. These predictions are obtained under the approximation [3,25] $\sigma_{SN}^2 \sim \sigma_{SS} \sigma_{NN}$, which is used to determine the cosmic S abundance. Such baryonic SIMPs fail to saturate halo dark matter for $\sigma_{SN} > 10^{-3}$ mb. The entries in boldface font are excluded by the present experimental results at the 95% confidence level. For the sake of comparison to Ref. [25] we assume here that $M'_X \approx M_S$.

M_X (GeV/c^2)	σ_{SN} (mb)									
	0.0005	0.0015	0.0042	0.012	0.032	0.09	0.25	0.69	1.9	5.3
2.7								5.9	7.9	8.3
4.3							5.7	7.7	8.1	11.1
7.1						5.5	7.5	7.9	10.9	12.1
12					5.6	7.6	8.1	8.5	12.2	12.7
19					7.5	7.9	8.3	11.3	12.5	12.9
31				7.4	7.8	8.2	8.6	12.4	12.8	13.2
50			5.7	7.7	8.1	8.5	11.5	12.7	13.1	13.6
81		5.7	7.7	8.1	8.5	8.9	11.9	13.1	13.5	14.0
132	5.7	7.7	8.1	8.5	8.9	9.3	12.2	13.5	13.9	14.3
220	6.0	8.0	8.4	8.9	9.3	9.7	12.6	13.9	14.3	14.7

Running at $q = +7$ we found $I_{det} = (4.8 \pm 0.1)$ nA for the lab gold, and $I_{det} = (4.7 \pm 0.1)$ nA for the Australian gold samples. As noted above the ratio of the transmission efficiency for the massive isotope to that of gold, η_X/η_{Au} , was found to vary with mass as can be seen from Fig. 1.

When the data in Figs. 1 and 2 are inserted into Eq. (1) we arrive at the limits on X/Au given in Tables II and III. The analysis performed on both the lab and Australia gold samples found no evidence for the presence of any anomalous gold nuclei for M_X in the range 186.3–325.9 GeV/c^2 . Figure 2 shows the limits set on the abundance of SIMPs in Au as a function of the effective SIMP mass M'_X . We define $M'_X \equiv M_X - M_{\text{Au}} = M_S - |E_B|$ where $|E_B|$ is the magnitude of the (unknown but presumably small) binding energy of the SIMP to the Au nucleus. Table II exhibits the X/Au ratios for both the lab gold and Australia gold at each of the masses predicted by those theories whose range is covered in the present experiment. We can display the constraints emerging from this scan on Table II of Ref. [25] by identifying the regions excluded by the present experiment. The boldface values in our Table III represent those entries for which the abundance of SIMPs in gold should have been large enough for SIMPs to have been seen by our AMS search had they been present.

This work was supported in part by the U.S. Department of Energy under Contract No. DE-AC02-76ER01428 and National Science Foundation Grant No. 9809983-EAR.

- [1] G. Jungman, M. Kamionkowski, and K. Griest, *Phys. Rep.* **267**, 195 (1996).
- [2] E. Nardi and E. Roulet, *Phys. Lett. B* **245**, 105 (1990).
- [3] R.N. Mohapatra and V.L. Teplitz, *Phys. Rev. Lett.* **81**, 3079 (1998); see also C.B. Dover, T.K. Gaisser, and G. Steigman, *ibid.* **42**, 1117 (1979); D.A. Dicus and V.L. Teplitz, *ibid.* **44**, 218 (1980).
- [4] S. Dimopoulos *et al.*, *Phys. Rev. D* **41**, 2388 (1990).
- [5] R.S. Chivukula *et al.*, *Phys. Rev. Lett.* **65**, 957 (1990).
- [6] R.N. Mohapatra and S. Nandi, *Phys. Rev. Lett.* **79**, 181 (1997).
- [7] S. Raby, *Phys. Rev. D* **56**, 2852 (1997); *Phys. Lett. B* **422**, 158 (1998).
- [8] Z. Chacko *et al.*, *Phys. Rev. D* **56**, 5466 (1997).
- [9] V. Berezhinsky and M. Kachelriess, *Phys. Lett. B* **422**, 163 (1998).
- [10] V.S. Berezhinskiĭ and B.L. Ioffe, *Zh. Eksp. Teor. Fiz.* **90**, 1567 (1986) [*Sov. Phys. JETP* **63**, 920 (1986)].
- [11] R.N. Mohapatra and S. Nussinov, *Phys. Rev. D* **57**, 1940 (1998).
- [12] I.F.M. Albuquerque, G.R. Farrar, and E.W. Kolb, *Phys. Rev. D* **59**, 015021 (1998).
- [13] D.J.H. Chung, G.R. Farrar, and E. W. Kolb, *Phys. Rev. D* **57**, 4606 (1998).
- [14] P.L. Biermann, *J. Phys. G* **23**, 1 (1997).
- [15] E.B. Norman, S.B. Gazes, and D.A. Bennett, *Phys. Rev. Lett.* **58**, 1403 (1987).
- [16] T.K. Hemmick *et al.*, *Phys. Rev. D* **41**, 2074 (1990).
- [17] G.D. Starkman *et al.*, *Phys. Rev. D* **41**, 3594 (1990).
- [18] E.W. Kolb and M. Turner, *The Early Universe* (Addison-Wesley, Reading, MA, 1990).
- [19] K. Greisen, *Phys. Rev. Lett.* **16**, 748 (1966).
- [20] G.T. Zatsepin and V.A. Kuz'min, *Zh. Eksp. Teor. Fiz., Pis'ma Red.* **4**, 114 (1966) [*JETP Lett.* **4**, 78 (1966)].
- [21] D. Elmore *et al.*, *Nucl. Instrum. Methods Phys. Res. B* **123**, 69 (1997).
- [22] D.L. Knies and D. Elmore, *Nucl. Instrum. Methods Phys. Res. B* **92**, 134 (1994).
- [23] H.D. Betz, *Rev. Mod. Phys.* **44**, 465 (1972).
- [24] Particle Data Group, R.M. Barnett *et al.*, *Phys. Rev. D* **54**, 1 (1996).
- [25] R.N. Mohapatra *et al.*, *Phys. Rev. D* **60**, 115013 (1999).